TOXICOLOGICAL SCIENCES **114(2)**, 323–334 (2010)
doi:10.1093/toxsci/kfp312
Advance Access publication January 4, 2010

Involvement of Caspase Activation in Azaspiracid-Induced Neurotoxicity in Neocortical Neurons

Zhengyu Cao,* Keith T. LePage,† Michael O. Frederick,‡ Kyriacos C. Nicolaou,‡,§ and Thomas F. Murray*,[1]

*Department of Pharmacology, School of Medicine, Creighton University, Omaha, Nebraska 68178; †Peptide Research Laboratories, Department of Medicine, Tulane University Medical Center, Tulane University, New Orleans, Louisiana 70112-2699; ‡Department of Chemistry and The Skaggs Institute for Chemical Biology, The Scripps Research Institute, La Jolla, California 92037; and §Department of Chemistry and Biochemistry, University of California, San Diego, La Jolla, California 92093

[1] To whom correspondence should be addressed. Fax: (402) 280-2142. E-mail: tfmurray@creighton.edu.

Received November 20, 2009; accepted December 26, 2009

Azaspiracids (AZAs) are a novel group of marine phycotoxins that have been associated with severe human intoxication. We found that AZA-1 exposure increased lactate dehydrogense (LDH) efflux in murine neocortical neurons. AZA-1 also produced nuclear condensation and stimulated caspase-3 activity with an half maximal effective concentration (EC_{50}) value of 25.8nM. These data indicate that AZA-1 triggers neuronal death in neocortical neurons by both necrotic and apoptotic mechanisms. An evaluation of the structure-activity relationships of AZA analogs on LDH efflux and caspase-3 activation demonstrated that the full structure of AZAs was required to produce necrotic or apoptotic cell death. The similar potencies of AZA-1 to stimulate LDH efflux and caspase-3 activation and the parallel structure-activity relationships of azaspiracid analogs in the two assays are consistent with a common molecular target for both responses. To explore the molecular mechanism for AZA-1–induced neurotoxicity, we assessed the influence of AZA-1 on Ca^{2+} homeostasis. AZA-1 suppressed spontaneous Ca^{2+} oscillations (EC_{50} = 445nM) in neocortical neurons. A distinct structure-activity profile was found for inhibition of Ca^{2+} oscillations where both the full structure as well as analogs containing only the FGHI domain attached to a phenyl glycine methyl ester moiety were potent inhibitors. The molecular targets for inhibition of spontaneous Ca^{2+} oscillations and neurotoxicity may therefore differ. The caspase protease inhibitor Z-VAD-FMK produced a complete elimination of AZA-1–induced LDH efflux and nuclear condensation in neocortical neurons. Although the molecular target for AZA-induced neurotoxicity remains to be established, these results demonstrate that the observed neurotoxicity is dependent on a caspase signaling pathway.

Key Words: **azaspiracid; apoptosis; caspase-3; neurotoxicity; neocortical neurons.**

Azaspiracids (AZAs) represent a novel class of marine phycotoxins that were originally identified following the reported cases of shellfish intoxication from mussels cultivated in Killary Harbor, Ireland (McMahon and Silke, 1996). Additional cases of shellfish intoxication associated with azaspiracids have more recently been reported in coastal European countries (James *et al*., 2002; Magdalena *et al*., 2003). Human symptoms of AZA intoxication include gastrointestinal symptoms, such as nausea, vomiting, diarrhea, and stomach cramps. These symptoms resemble those of diarrhetic shellfish poisoning caused by okadaic acid and dinophysistoxins. In mice and rats ip injection of AZA also produces neurological symptoms with progressive paralysis, fatigue, difficulty breathing, and subsequent lethality (McMahon and Silke, 1996).

Since the isolation of azaspiracid-1 (AZA-1) in 1998 (Satake *et al*., 1998), more than 20 distinct azaspiracid (AZA) analogs have been identified (Furey *et al*., 2002; James *et al*., 2002; Ofuji *et al*., 2001). AZA-1, AZA-2, and AZA-3 are the predominant AZA analogs in nature (James *et al*., 2002). The total synthesis by the Nicolaou group indicated that the structure originally proposed by Satake *et al*. (1998) was incorrect (Nicolaou *et al*., 2006b). While the polyether backbone of AZA is similar to other classes of marine toxins, the AZAs are characterized by unusual structural motifs including spiro-ring assemblies, a secondary amino group, and a carboxylic acid moiety, making them unique within the nitrogen-containing marine toxins (Satake *et al*., 1998). Through both degradative and synthetic means, the Nicolaou group has synthesized the correct structure of AZA-1 (Nicolaou *et al*., 2004a,b, 2006a,b,c) as well as AZA-2 and -3 (Nicolaou *et al*., 2006d).

While the scarcity of purified AZAs has hampered efforts to characterize the pharmacological properties of this toxin, progress has been made in recent years. Oral administration of AZA-1 subacutely produced multiple organ system damage, including necrosis of the lamina propria of the small intestine and in the lymphoid tissues such as thymus, spleen, and the Peyer's patches (Ito *et al*., 2000). Chronic effects of sublethal dosages of AZA-1 in mice were found to include erosion and shortened villi in the stomach and small intestine, fatty changes in the liver, extreme weakness, interstitial pneumonia, the

appearance of lung tumors, and hyperplasia of epithelia in the stomach (Ito *et al*., 2002).

In vitro studies have been performed to explore the mode of action of AZAs. AZA-1 has been demonstrated to be toxic to several mammalian cell types at low nanomolar concentrations (Twiner *et al*., 2005). In human T lymphocytes, AZAs produced elevations of intracellular Ca^{2+} and cyclic adenosine monophosphate levels (Alfonso *et al*., 2005; Roman *et al*., 2002, 2004), while in human neuroblastoma cells, AZA-1 produced irreversible cytoskeletal disarrangement that was independent of caspase activity (Vilarino *et al*., 2007). In cerebellar granule cells (CGCs), AZA-1 elevated intracellular Ca^{2+}; however, this did not account for AZA-1–induced neurotoxicity (Vale *et al*., 2007a). In a spinal cord neuronal network, AZA-1 inhibited bioelectrical activity without significant effect on voltage-gated sodium or calcium currents, suggesting that the toxin affects synaptic transmission in neuronal network through a mechanism independent of the voltage-gated channels (Kulagina *et al*., 2006). Recently, Vale *et al*. (2007b) reported that AZA-1 stimulated c-Jun-N-terminal kinase (JNK) activity. Additionally, application of the JNK inhibitor, SP 600125, inhibited AZA-1–induced toxicity in CGCs. These data suggested the involvement of JNK activity in AZA-1–induced neurotoxicity. However, the molecular target and toxicological mechanism of action of AZA-induced neurotoxicity remain to be established.

Ca^{2+} oscillations play an important physiologic role in the nervous system. Ca^{2+} oscillations have been reported in neocortical, hippocampal, and cerebellar granule neurons (Dravid and Murray, 2004; Nunez *et al*., 1996; Ogura *et al*., 1987). These spontaneous Ca^{2+} oscillations have been implicated in the regulation of neuronal plasticity in developing neurons (Spitzer *et al*., 1995). Ca^{2+} spikes also promote neurotransmitter receptor expression and ion channel maturation in *Xenopus* embryonic neurons (Gu and Spitzer, 1995) and modulate neuronal migration in cerebellar granule neurons (Komuro *et al*., 1996).

Herein, we have examined the influence of AZAs on spontaneous Ca^{2+} oscillations and neurotoxicity in neocortical neurons. We demonstrate that AZA-induced neurotoxicity includes both necrotic and apoptotic cell death. An evaluation of the structure-activity relationships of AZA analogs furthermore demonstrated that the full structure of AZA is required for producing neurotoxicity in neocortical neurons. In contrast, a distinct structure-activity profile was found for inhibition of spontaneous Ca^{2+} oscillations where both the full structure as well as analogs containing the FGHI domain attached to a phenyl glycine methyl ester moiety were potent inhibitors.

MATERIALS AND METHODS

Materials. Trypsin, penicillin, streptomycin, heat-inactivated fetal bovine serum, horse serum, and soybean trypsin inhibitor were obtained from Atlanta Biologicals (Norcross, GA). Minimum essential medium (MEM), deoxyribonuclease (DNase), poly-L-lysine, cytosine arabinoside, Hoechst 33342, MK-801, nifedipine, and β-nicotinamide adenine dinucleotide were from Sigma (St Louis, MO). The sodium sensitive fluorescent dye SBFI, pluronic acid F-127, and caspase-3 activity assay kit were obtained from Invitrogen Corporation (Carlsbad, CA). Tetrodotoxin (TTX) was purchased from Tocris Cookson, Inc. (Ellisville, MO). Stress-activated protein kinase/c-Jun N-terminal kinase (SAPK/JNK) antibody and anti-phospho-SAPK/JNK (Thr183/Tyr185) were from Cell Signaling Technology (Danvers, MA). SP 600125, Ac-DEVD-CMK, and Z-VAD-FMK were from Biomol International (Plymouth Meeting, PA).

Synthesis of azaspiracid. The synthesis of azaspiracid-1 (1) and analogs (2–14) have been described by Nicolaou *et al*. (2006c). The structures of AZA-1 (1) as well as the derivatives (2–15) examined in this study are illustrated in Figure 1.

Toxin exposure. AZA analogs were dissolved in dimethyl sulfoxide (DMSO) at a stock concentration of 10mM. Neocortical neurons at days *in vitro* (DIV) 8–10 were used. All assays were carried out in the presence of 0.1% DMSO, which by itself was without effect on the assays used in this study. The inhibitors and antagonists were added 1 h prior to the addition of AZA-1.

Neocortical neuron culture. Primary cultures of neocortical neurons were obtained from embryonic days 16–17 Swiss-Webster mice and processed as previously described (Cao *et al*., 2007). Briefly, pregnant mice were euthanized by CO_2 asphyxiation, and embryos were removed under sterile conditions. Neocortices were collected, stripped of meninges, minced by trituration with a Pasteur pipette, and treated with trypsin for 25 min at 37°C. The cells were then dissociated by two successive trituration and sedimentation steps in soybean trypsin inhibitor and DNase containing isolation buffer, centrifuged, and resuspended in Eagle's MEM with Earle's salt supplemented with 1mM L-glutamine, 10% fetal bovine serum, 10% horse serum, 100 IU/ml penicillin, and 0.10 mg/ml streptomycin, pH 7.4. Cells were plated onto poly-L-lysine–coated, 96-well, clear-bottomed, black-well culture plates (Corning Life Science, Acton, MA) at a density of 1.5×10^5 cells/well. Cells were incubated at 37°C in a 5% CO_2 and 95% humidity atmosphere. Cytosine arabinoside (10μM) was added to the culture medium on day 2 after plating to prevent proliferation of nonneuronal cells. The culture medium was changed on days 5, 7, and 9 using Neurobasal medium supplemented with B-27, 0.2mM L-glutamine, 100 IU/ml penicillin, and 0.10 mg/ml streptomycin, pH 7.4. The cultures were used for experiments between 8 and 13 DIV. All animal use protocols were approved by the Institutional Animal Care and Use Committee.

Intracellular Ca^{2+} monitoring. Neocortical neurons grown in 96-well plates were used for $[Ca^{2+}]_i$ measurements at 12–13 DIV. Briefly, the growth medium was removed and replaced with dye loading buffer (50 μl/well) containing 4μM fluo-3 and 0.04% pluronic acid F-127 in Locke's buffer (8.6mM 4-(2-hydroxyethyl)-1-piperazineethanesulfonic acid, 5.6mM KCl, 154mM NaCl, 5.6mM glucose, 1.0mM $MgCl_2$, 2.3mM $CaCl_2$, and 0.0001mM glycine, pH 7.4). After 1-h incubation in dye loading buffer, the neurons were washed four times in fresh Locke's buffer (200 μl/well) using an automated cell washer (BioTek Instrument, Inc., Winooski, VT) and transferred to a Fluorescence Laser Plate Reader (FLIPR) (Molecular Devices, Sunnyvale, CA) incubation chamber. The final volume of Locke's buffer in each well was 150 μl. Neurons were excited by the 488-nm line of the argon laser, and Ca^{2+}-bound fluo-3 emission in the 500–600 nm range was recorded with the charge-coupled device (CCD) camera with shutter speed set at 0.4 s. FLIPR operates by illuminating the bottom of a 96-well microplate with an argon laser and measuring the fluorescence emissions in all 96 wells simultaneously using a cooled CCD camera. Different concentrations of AZAs were added to neurons after a 5-min baseline recording from a compound plate in a volume of 50 μl at the rate of 30 μl/s. Fluorescence readings were taken every 2 s over a 30-min experimental time period.

Lactate dehydrogense activity assay. Neocortical neurons cultured in 96-well plates were used for lactate dehydrogense (LDH) efflux assay. All assays were carried out in the presence of 0.1% DMSO, which by itself has no effect on LDH efflux in neocortical neurons. Neocortical neurons (DIV 8) were continuously exposed to the desired concentrations of AZA analogs in the culture medium. The medium was collected after toxin exposure for various times and assayed for LDH activity. LDH activity was determined

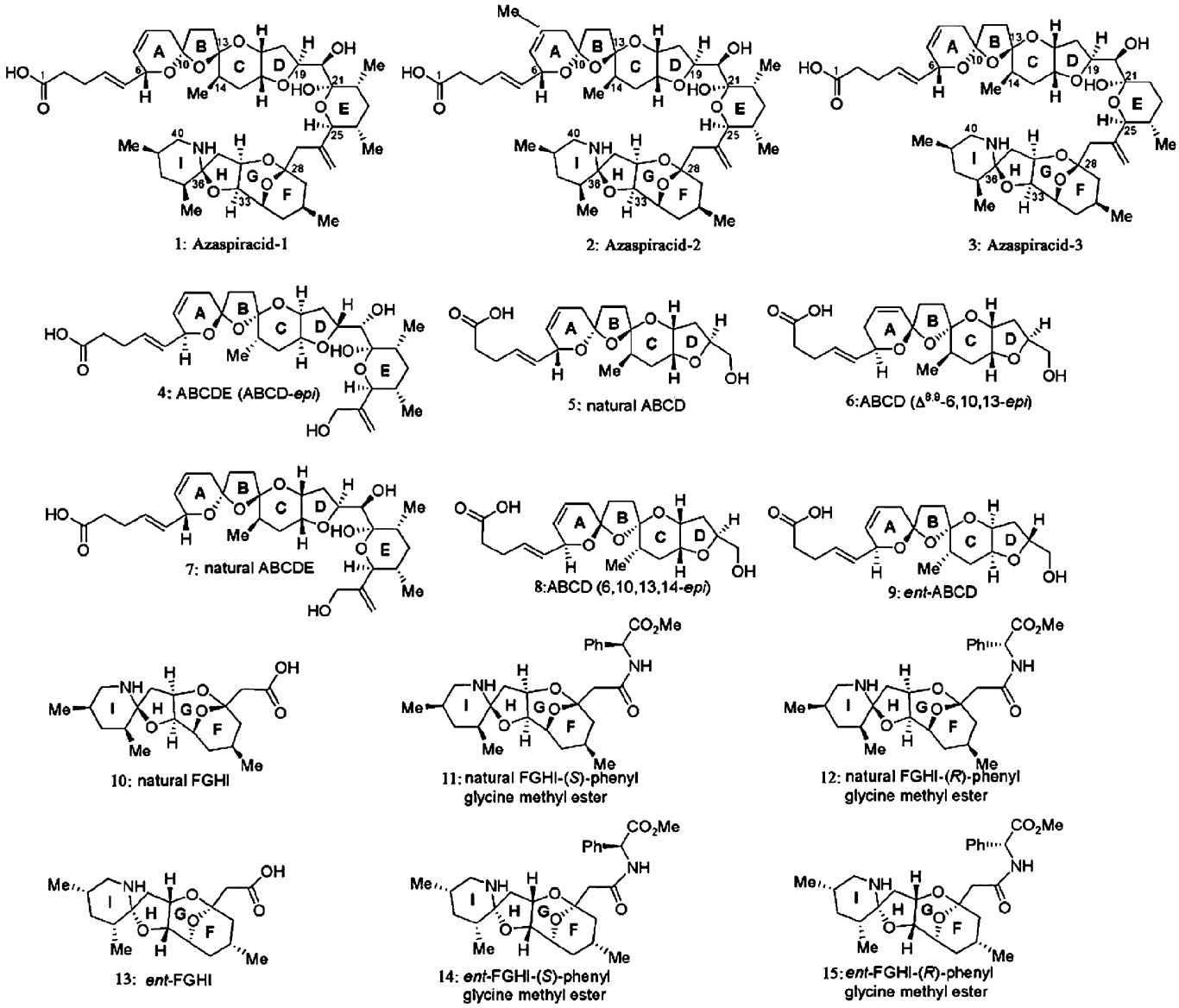

FIG. 1. The structures of AZA-1 (1) and analogs 2–15.

spectrophotometrically as described by Koh and Choi (1987). These data are reported as LDH activity units per plate or normalized to percentage of maximum LDH activity resulted from H_2O cell lysate.

Hoechst 33342 staining. Neocortical neurons cultured in 96-well plates (DIV 8) were exposed to a range of AZAs concentrations for the indicated times. The medium was then aspirated and a concentration of 1.6 μg/ml of Hoechst 33342 dye (cell permeable) in Locke's buffer was added to the neocortical neurons. The neurons were then incubated for 15 min at 37°C in the dark. Images were then taken using an Olympus IX71 confocal microscope.

Caspase-3 activity assay. Neocortical neurons cultured in 96-well plates (DIV 8) were treated with AZA-1 for the desired time. The cells were then washed three times with PBS and lysed in 60 μl lysis buffer (20mM Tris, 100mM NaCl, 0.5mM EDTA, and 0.01% Triton X-100, pH 7.5). After centrifugation for 10 min at 5000 × g, the supernatant (40 μl) was mixed with equal volume of 2× reaction buffer (20mM piperazine-1,4-bis(2-ethanesulfonic acid), 4mM EDTA, 0.2% 3[(3-Cholamidopropyl)dimethylammonio]-propane-sulfonic acid, and 10μM dithiothreitol, pH 7.4) containing 25μM of a fluorometric substrate, bisamide derivative of rhodamine 110 (Z-DEVD-R110), and incubated in the dark for 20–40 min at room temperature. The fluorescent products, monoamide R110 (R110), were determined using a FLEXstation II (Molecular Devices) by measuring emission fluorescence at 525 nm with 480 nm excitation. Caspase-3 activity was determined from the cleavage of Z-DEVD-R110 to the fluorescent product, R110.

Western blotting. Cells were washed three times with Locke's buffer and then allowed to equilibrate in Locke's for 15 min. After this period, cultures were treated with 1μM AZA-1 diluted in Locke's buffer and incubated at 37°C for specified times. Cultures were then transferred to an ice slurry to terminate treatment. After washing with ice-cold PBS, cells were harvested in ice-cold lysis buffer containing 50mM Tris, 50mM NaCl, 2mM EDTA, 2mM ethylene glycol tetraacetic acid, 1% Nonidet P40, 2.5mM sodium pyrophosphate, 1mM sodium orthovanadate, 1 μg/ml leupeptin, 1 μg/ml aprotinin, 1 μg/ml pepstatin,

and 1mM phenylmethylsulfonyl fluoride just prior to use and incubated for 20 min at 4°C. Cell lysates then underwent sonication and were centrifuged at 16,000 × g for 10 min at 4°C. The supernatant obtained after centrifugation of lysates was assayed by the Bradford method to determine protein content. Equal amounts (30 μg) of protein were mixed with the Laemmli sample buffer and boiled for 5 min. The samples were loaded onto a 12% SDS-polyacrylamide gel electrophoresis gel and transferred to a nitrocellulose membrane by electroblotting. The membranes were blocked in TBST (20mM Tris, 150mM NaCl, and 0.1% Tween 20) with 5% skimmed milk for 1 h at room temperature. After blocking, membranes were incubated overnight at 4°C in primary antibody diluted in TBST containing 5% skimmed milk. The blots were washed and incubated with the secondary antibody conjugated with horseradish peroxidase for 1 h, washed four times in TBST, and exposed with ECL Plus for 3 min. Blots were exposed to Kodak Hyperfilm and developed. Membranes were stripped with stripping buffer (63mM Tris base, 70mM SDS, and 0.0007% 2-mercaptoethanol, pH 6.8) and reblotted for further use.

Data analysis. Quantification of Ca^{2+} oscillation data was achieved by counting the number of Ca^{2+} oscillations beginning 15 min after azaspiracid exposure for a period of 10 min. Concentration-response data were analyzed by nonlinear regression analysis with the GraphPad software (Version 4.0, San Diego, CA). Statistical significance was determined by an ANOVA and, where appropriate, a Dunnett's multiple comparison test was performed to compare responses of vehicle and AZAs-treated neurons.

RESULTS

Cytotoxic Effect of AZA-1 on Neocortical Neurons

AZA-1 exposure produced neurotoxicity in neocortical neurons. Neocortical neurons exposed to AZA-1 for 2 h did not display significant neuron death. However, after a 12-h treatment, AZA-1 produced neuronal death as reflected in elevated levels of LDH efflux. This AZA-1 neurotoxicity was concentration dependent with an EC_{50} value of 221.0nM (95% confidence interval [95% CI] 78.5–622.6). The maximum LDH activity was 18.5% of the total cell lysis LDH value (Fig. 2a). Neocortical neurons exposed to AZA-1 for 24, 48, and 72 h displayed progressively larger toxic insults with EC_{50} values of 111.3nM (64.5–191.8, 95% CI), 41.1nM (17.2–98.3, 95% CI), and 34.2nM (24.2–48.1, 95% CI), respectively, and maximum LDH activities of 25.6, 36.9, and 42.4% of the total cell lysis value, respectively (Fig. 2a).

Cytotoxic Effects of Azaspiracid Analogs on Neocortical Neurons

Given the demonstration of AZA-1 neurotoxicity in neocortical neurons, we next examined the structure-activity relationships for 15 synthesized AZA analogs on LDH efflux. We exposed cultured neocortical neurons to a concentration of 1μM of each analog for 48 h. As illustrated in Figure 2b, analogs containing both the ABCDE and the FGHI domains including AZA-1 (1), AZA-2 (2), and AZA-3 (3) increased LDH efflux in neocortical neurons, while fragments containing either the ABCDE domain or the FGHI domain alone were without effect on LDH efflux. Given the observed cytotoxicity to neocortical neurons exposed to 1μM

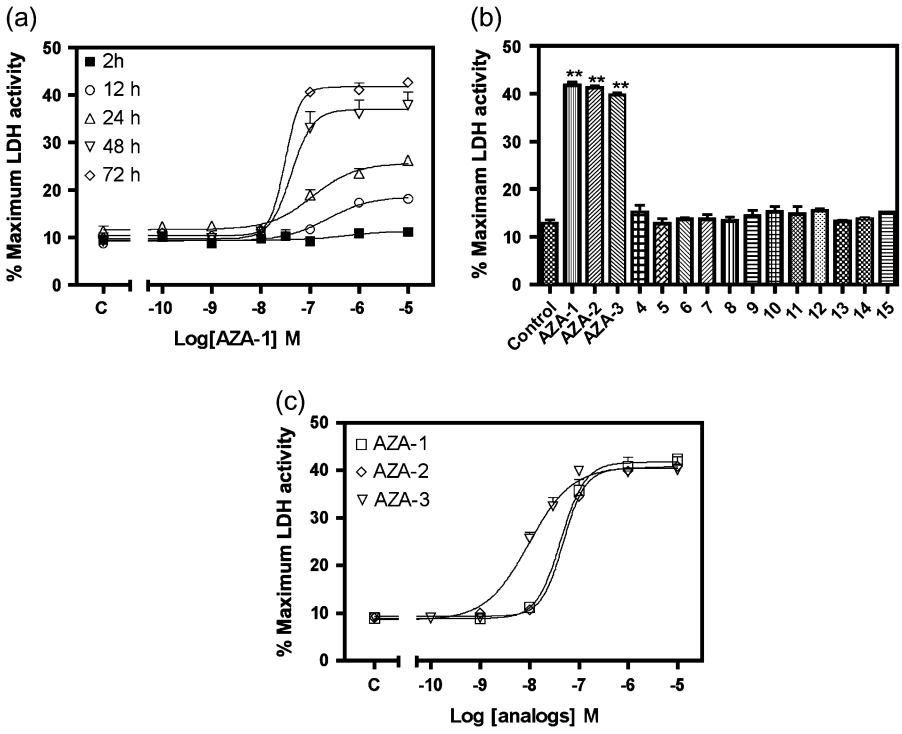

FIG. 2. (a) Neurotoxic concentration-response profiles of neocortical neurons exposed for 2, 24, 48, and 72 h to AZA-1. (b) The effects of AZA analogs (1μM) on LDH efflux in neocortical neurons (**$p < 0.01$, AZAs vs. control). (c) Neurotoxic concentration-response profiles for neocortical neurons exposed for 48 h to AZA-1, AZA-2, and AZA-3. LDH activity was determined as described in the ''Materials and Methods'' section. Individual points represent the mean ± SEM from at least three separate experiments performed in duplicate.

of AZA-2 and AZA-3, we then compared the potencies of AZA-1, AZA-2, and AZA-3 on LDH efflux. Exposure of neocortical neurons to AZA-1, AZA-2, or AZA-3 for 48 h resulted in a concentration-dependent increase in LDH efflux (Fig. 2c). The EC_{50} values were 42.7nM (29.8–69.0, 95% CI), 48.0nM (33.4–69.0, 95% CI), and 9.88nM (7.77–12.55, 95% CI) for AZA-1, AZA-2, and AZA-3, respectively. The efficacies of AZA-1, AZA-2, and AZA-3 on LDH efflux did not differ.

Effect of AZA-1 on Spontaneous Ca^{2+} Oscillations in Neocortical Neurons

Neocortical neurons in culture develop extensive processes and form a synaptically connected network that generates spontaneous Ca^{2+} oscillations (Dravid and Murray, 2004). These spontaneous Ca^{2+} oscillations afford an extremely sensitive assay for drug or neurotoxin influence on neuronal signaling. We therefore assessed the influence of AZAs on neocortical neuron Ca^{2+} oscillations. AZA-1 treatment decreased both the frequency and amplitude of spontaneous Ca^{2+} oscillations in a concentration-dependent manner in neocortical neurons (Fig. 3). The AZA-1–induced inhibition of spontaneous Ca^{2+} oscillations began ~1 min after addition to the culture (data not shown). The Ca^{2+} oscillation frequency was determined 15 min after addition of AZA-1 for a period of 10 min. The AZA-1 concentration-response data were best fit by a three-parameter logistic equation yielding an EC_{50} value of 445nM (337–587, 95% CI) (Fig. 4a).

Effects of Azaspiracid Analogs on Spontaneous Ca^{2+} Oscillations

We then examined the structure-activity relationships of AZA analogs as inhibitors of spontaneous Ca^{2+} oscillations in neocortical neurons. Given the complete inhibition of Ca^{2+} oscillations by 10μM of AZA-1, we exposed cultured neocortical neurons to a concentration of 10μM of each analog. As depicted in Figure 4b, addition of AZA-1 (1), AZA-2 (2), and AZA-3 (3), analogs that contain both the ABCDE and the FGHI domains, resulted in complete or nearly complete suppression of oscillations. Interestingly, addition of fragments 11, 12, 14, and 15 possessing only the FGHI domain attached to a phenyl glycine methyl ester moiety also were effective inhibitors of spontaneous Ca^{2+} oscillations in neocortical neurons. Given these inhibitory effects on spontaneous Ca^{2+} oscillations by AZA-1 (1), AZA-2 (2), AZA-3 (3), and fragments 11, 12, 14, and 15, we next ascertained the concentration-response relationships of these compounds as inhibitors of spontaneous Ca^{2+} oscillations. All analogs tested produced concentration-dependent inhibition of oscillations (Fig. 4c). The relative potencies (EC_{50} values) of these analogs as inhibitors of spontaneous Ca^{2+} oscillations are summarized in Table 1. AZA-3 proved to be the most potent analog, with AZA-2 and AZA-1 having somewhat lower potencies as inhibitors of spontaneous Ca^{2+} oscillations. The rank order of potencies of the tested AZA analogs was AZA-3 > AZA-2 > AZA-1 > 12 > 11 = 15 > 14.

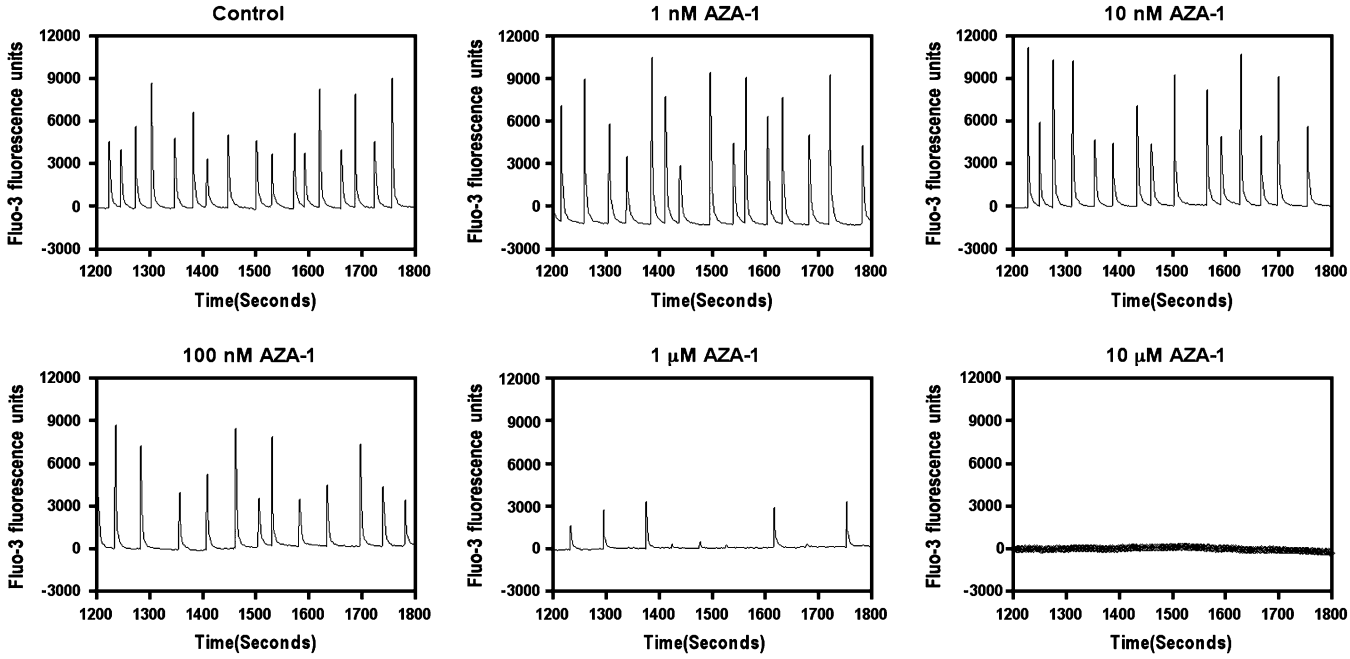

FIG. 3. Time- and concentration-response data for AZA-1–induced suppression of spontaneous Ca^{2+} oscillations in neocortical neurons.

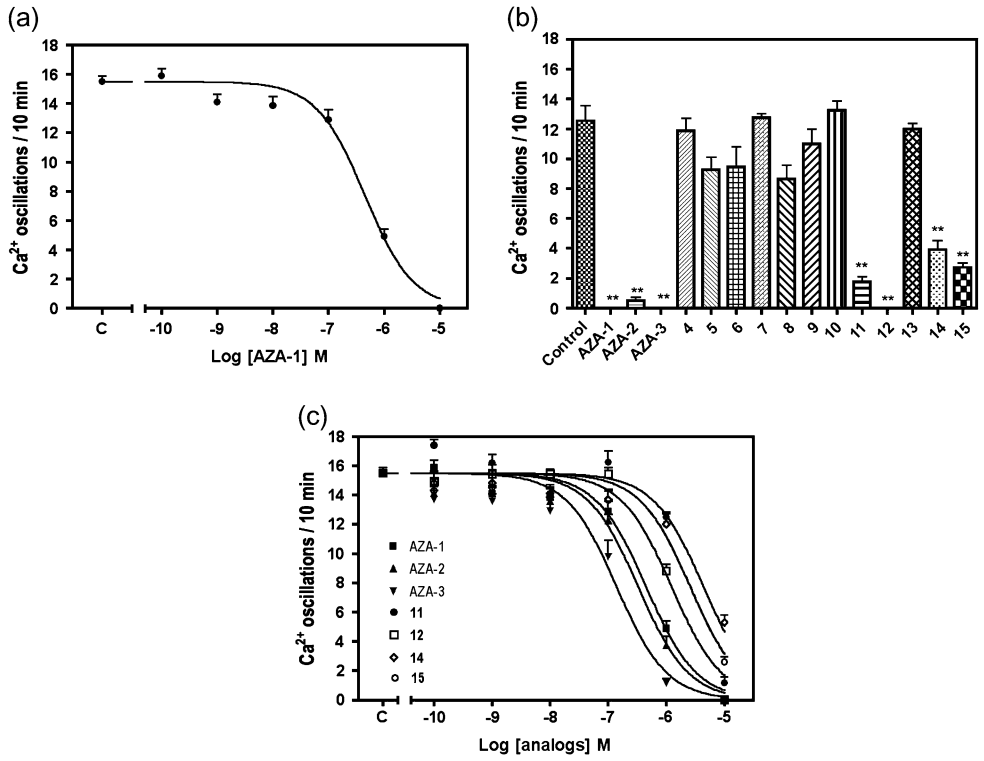

FIG. 4. (a) Concentration-response relationships for AZA-1–induced suppression of spontaneous Ca^{2+} oscillations in neocortical neurons. The number of spikes was derived from a 10-min exposure period beginning 15 min after addition of AZA-1. (b) Effects of AZA analogs (10μM) on spontaneous Ca^{2+} oscillations in neocortical neurons (**$p < 0.01$, AZAs vs. control). (c) Concentration-response relationships for AZA analog–induced suppression of spontaneous Ca^{2+} oscillations in neocortical neurons. Each data point represents mean ± SEM from at least three independent experiments performed in triplicate.

Effect of AZA-1 on Caspase-3 Activity on Neocortical Neurons

Apoptosis and necrosis are generally recognized as two distinct pathways of cell death. Given that LDH efflux represents a useful assay for necrotic cell death, we asked further whether AZAs are capable of producing apoptotic cell death in neocortical neurons. Caspase proteases play a critical role in apoptotic neuronal death, and the activation of caspases has been considered to be an early marker of apoptotic cell death. We accordingly tested the influence of AZA-1 on caspase-3 activity in neocortical neurons. Caspase-3 activity was significantly enhanced as early as 8 h after treatment with AZA-1 (1μM), and this response increased with time (Fig. 5a). As depicted in Figure 5b, treatment with AZA-1 for 24 h produced a robust and concentration-dependent stimulation of caspase-3 activity with an EC_{50} value of 25.8nM (17.6–37.7, 95% CI).

TABLE 1
Potencies of AZA Analogs as Inhibitors of Spontaneous Ca^{2+} Oscillations in Neocortical Neurons

	EC_{50} (nM)	95% CI (nM)
AZA-1	445.1	341.4–580.3
AZA-2	325.0	246.5–428.5
AZA-3	138.3	96.4–198.5
Compound 11	2,550	1,802–3,610
Compound 12	1,218	958.1–1,549
Compound 14	4,336	2,977–6,314
Compound 15	2,560	1,749–3,748

Effects of Azaspiracid Analogs on Caspase-3 Activity

We next evaluated the effects of the 15 AZA analogs on caspase-3 activity. The cultured neocortical neurons were exposed to a concentration of 1μM of each analog for 24 h. As depicted in Figure 5c and consonant with the structure-activity relationships for LDH efflux, only the analogs that contain both ABCDE and FGHI domains such as AZA-1, AZA-2, and AZA-3 stimulated caspase-3 activation. The fragments containing either the ABCDE domain alone or only the FGHI domain were without effect on caspase-3 activity.

Effect of AZA-1 on Nuclear/Chromatin Morphological Change on Neocortical Neurons

An additional characteristic of apoptotic cell death is nuclear/chromatin morphological changes that manifest as nuclear condensation. We therefore evaluated the effects of AZA-1 on nuclear morphology in neocortical neurons.

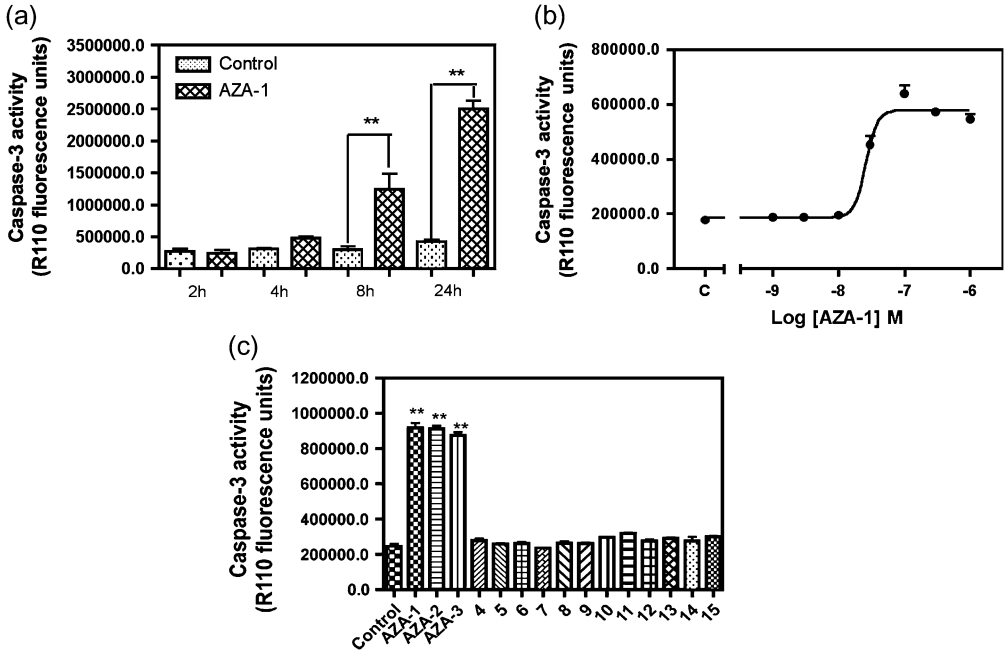

FIG. 5. (a) Time-response relationships for AZA-1–induced caspase-3 activation in neocortical neurons. The neocortical neurons were exposed to 1μM AZA-1 and caspase-3 activity determined as described in the ''Materials and Methods'' section. These experiments were repeated three times each in triplicate with similar results (**$p < 0.01$, AZA-1 vs. control). (b) Concentration-response relationships of AZA-1–induced caspase-3 activation. The neocortical neurons were exposed 24 h to AZA-1 (1nM–1μM). The EC_{50} value was 25.8nM (17.6–37.7, 95%CI). (c) The effects of AZA analogs on caspase-3 activity. Neocortical neurons were exposed to azaspiracid analogs (1μM) for 24 h (**$p < 0.01$, AZAs vs. control). These experiments were repeated three times each in triplicate with similar results.

Neocortical neurons displayed statistically significant nuclear morphological changes as early as 8 h after exposure to 1μM AZA-1. The percentage of apoptotic cells by this measure gradually increased and reached a peak response at 24 h of exposure. The percentage of apoptotic cells increased from 6.6 ± 0.5% to 62.6 ± 3.4% following 24-h exposure to 1μM AZA-1 (mean ± SEM, $p < 0.01$) (Fig. 6).

The Effects of the Caspase Inhibitors, Ac-DEVD-CMK and Z-VAD-FMK, on AZA-1–Induced Neurotoxicity in Neocortical Neurons

Given the enhanced caspase-3 activity, we next investigated whether a caspase-3 inhibitor could prevent the AZA-1–induced neurotoxicity in neocortical neurons. Neocortical neurons were pretreated with the caspase-3 inhibitor, Ac-DEVD-CMK (50μM), for 1 h before exposure to AZA-1 (1μM). This inhibitor efficiently suppressed AZA-1–induced caspase-3 activity (Supplementary fig. 1). Pretreatment with 50μM Ac-DEVD-CMK, which independently did not affect nuclear morphology or LDH efflux, produced a modest, yet statistically significant, reduction of AZA-1–induced nuclear condensation (Fig. 7a) and LDH efflux (Fig. 7b). It has been previously demonstrated that AZA-1 stimulated caspase-1 and caspase-3 to -9 activation in human neuroblastoma cells (Vilarino *et al.*, 2007). Given the partial protective effect of a caspase-3 inhibitor on AZA-1–induced neurotoxicity, we therefore evaluated the role of a broad-spectrum caspase inhibitor, Z-VAD-FMK. Pretreatment with Z-VAD-FMK (100μM) for 1 h prior to addition of 1μM of AZA-1 produced a nearly complete inhibition of AZA-1–induced nuclear condensation (Fig. 7a and Supplementary fig. 2) and LDH efflux (Fig. 7b).

Lack of Effect of Tetrodotoxin (TTX), MK-801, and Nifedipine on AZA-1–Induced Neurotoxicity in Neocortical Neurons

To further explore the molecular mechanisms responsible for AZA-1–induced neurotoxicity, we evaluated the roles of voltage-gated sodium channels (VGSCs), NMDA receptors, and L-type Ca^{2+} channels as targets for AZA-1. Application of the VGSC blocker (TTX, 1μM), the NMDA receptor antagonist (MK-801, 1μM), or the L-type Ca^{2+} channel antagonist (nifedipine, 1μM) for 1 h prior to the addition of AZA-1 (1μM) did not affect AZA-1–induced LDH efflux or nuclear/chromatin condensation in neocortical neurons (Supplementary fig. 3). These data therefore exclude VGSCs, NMDA receptors, and L-type Ca^{2+} channels as potential targets for AZA-1–induced neurotoxicity and are consistent with an earlier report that AZA-1 did not affect VGSC or voltage-gated calcium channel currents (Kulagina *et al.*, 2006).

The Effect of the JNK Inhibitor, SP 600125, on AZA-1–Induced Neurotoxicity in Neocortical Neurons

Inasmuch as it has been shown previously that AZA-1–induced JNK activation accounts for AZA-1–induced neurotoxicity in CGCs (Vale *et al.*, 2007b), we explored the involvement of the MAP kinase JNK in AZA-1–induced

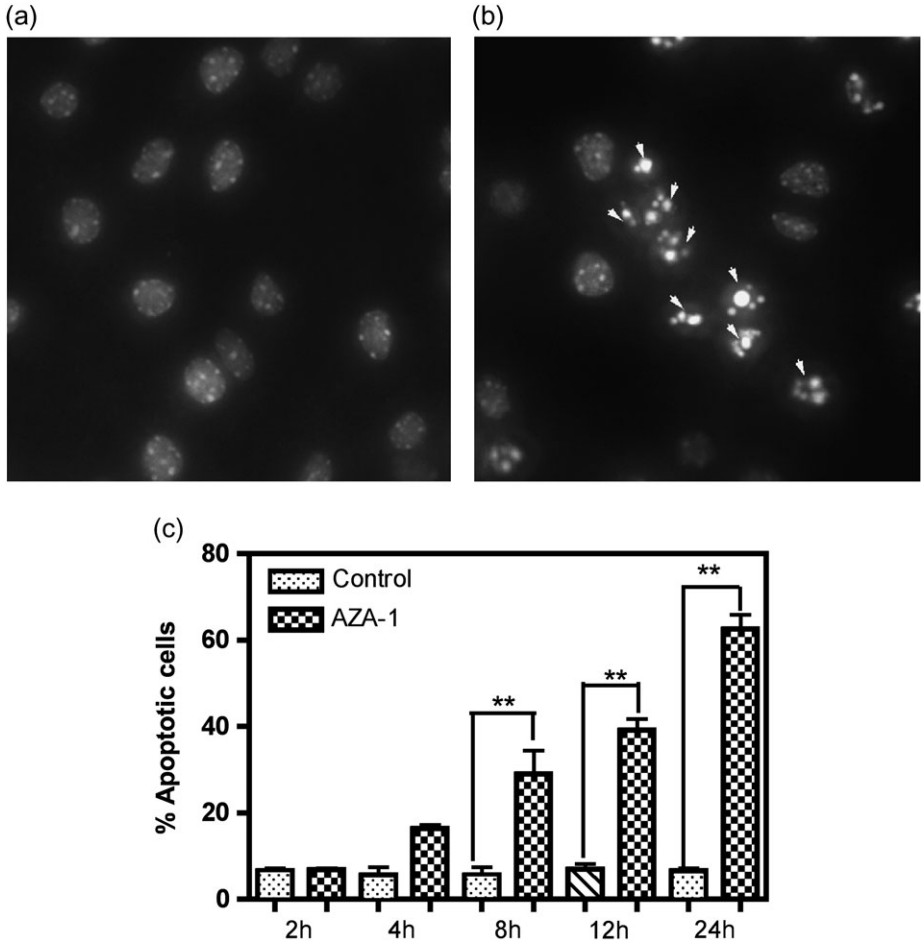

FIG. 6. Effect of AZA-1 on nuclear morphological changes in neocortical neurons. (a) Representative control neocortical neurons after exposure to 0.1% DMSO for 24 h. (b) Neurons exposed to 1μM azaspiracid-1. Neocortical neurons with condensed nuclei were revealed with Hoechst 33342 dye staining and marked with arrows. (c) Quantification of apoptotic neocortical neurons as detected by Hoechst 33342 staining after exposure to 0.1% DMSO or 1μM azaspiracid-1 for 2, 4, 8, and 24 h. These data are presented as the percentage of apoptotic cells and were obtained from three independent experiments performed in triplicate (**$p < 0.01$, AZA-1 vs. control).

neurotoxicity in neocortical neurons. Neocortical neurons were pretreated with the JNK inhibitor, SP 600125 (10μM), for 1 h prior to the addition of AZA-1. In contrast to the protective effect of JNK inhibition against AZA-induced neurotoxicity in CGCs, pretreatment of SP 600125 was without effect on both AZA-1–induced caspase-3 activity and LDH efflux (Figs. 8a and 8b). These data suggest that JNK is not involved in AZA-1–induced neurotoxicity in neocortical neurons. To confirm this, we directly assessed JNK phosphorylation after AZA-1 exposure. AZA-1 did not affect JNK phosphorylation, further demonstrating the lack of involvement of this MAP kinase pathway in AZA-1–induced neurotoxicity in neocortical neurons (Figs. 8c and 8d).

DISCUSSION

Although efforts have been made to understand the mechanisms of AZA-induced toxicity in a variety of cell lines and primary cultures of CGCs, the toxicological mechanism and molecular target(s) are still unclear (Roman *et al*., 2002; Twiner *et al*., 2005; Vale *et al*., 2007a). Our results demonstrate that AZA-1 neurotoxicity generalizes to neocortical neurons. AZA-1 produced cytotoxicity in a concentration- and time-dependent manner. A prolonged incubation time of 48 h was required for AZA-1 to produce a maximum level of cytotoxicity in neocortical neurons. This somewhat delayed neurotoxic response to AZA-1 in neocortical neurons is consistent with previous observations that demonstrated a requirement for prolonged exposures (>24 h) for substantial cytotoxicity and necrotic cell death in several cell lines and CGCs (Twiner *et al*., 2005; Vale *et al*., 2007a). A recent report has, however, indicated that short AZA-1 exposure periods were sufficient to produce alterations cytoskeleton morphology (Vilarino *et al*., 2007). This report found that AZA-1 exposure periods as short as 2 min were sufficient to disrupt cytoskeleton morphology in a human neuroblastoma cell line. This

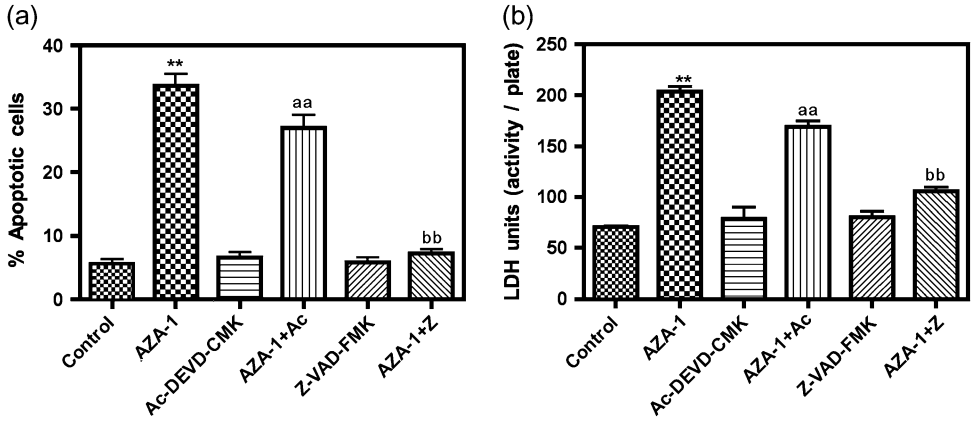

FIG. 7. (a) Effect of Ac-DEVD-CMK (50μM) and Z-VAD-FMK (100μM) on 1μM AZA-1–induced nuclear condensation and (b) effect of Ac-DEVD-CMK (50μM) and Z-VAD-FMK (100μM) on 1μM AZA-1–induced LDH efflux. These data were obtained from two independent cell cultures performed in triplicate (**$p < 0.01$, AZA-1 vs. control; aa, $p < 0.01$, AZA-1 + Ac vs. AZA-1; and bb, $p < 0.01$, AZA-1 + Z vs. AZA-1).

disruption of cytoskeletal morphology developed slowly with changes in cellular structure appearing at 24–48 h after the brief AZA-1 exposure period. We have also found that AZA-1 exposure of neocortical neuron for periods as short as 30 min is sufficient to produce a delayed neurotoxicity at 24 h (data not shown).

AZA-1 has been shown to produce neurotoxic effects in CGCs with an EC_{50} value in the low nanomolar range (Vale *et al.*, 2007a). We demonstrate here that AZA-1 produced substantial neurotoxicity with an EC_{50} value of 31.7nM (72-h treatment) in neocortical neurons. Collectively, these data indicate that AZA-1 is a potent (nanomolar) neurotoxin in both neocortical and cerebellar granule neurons. It is noteworthy that *in vivo* observations with mice and rats receiving ip injection of AZA demonstrate the production of neurological symptoms, such as progressive paralysis, fatigue, and difficulty

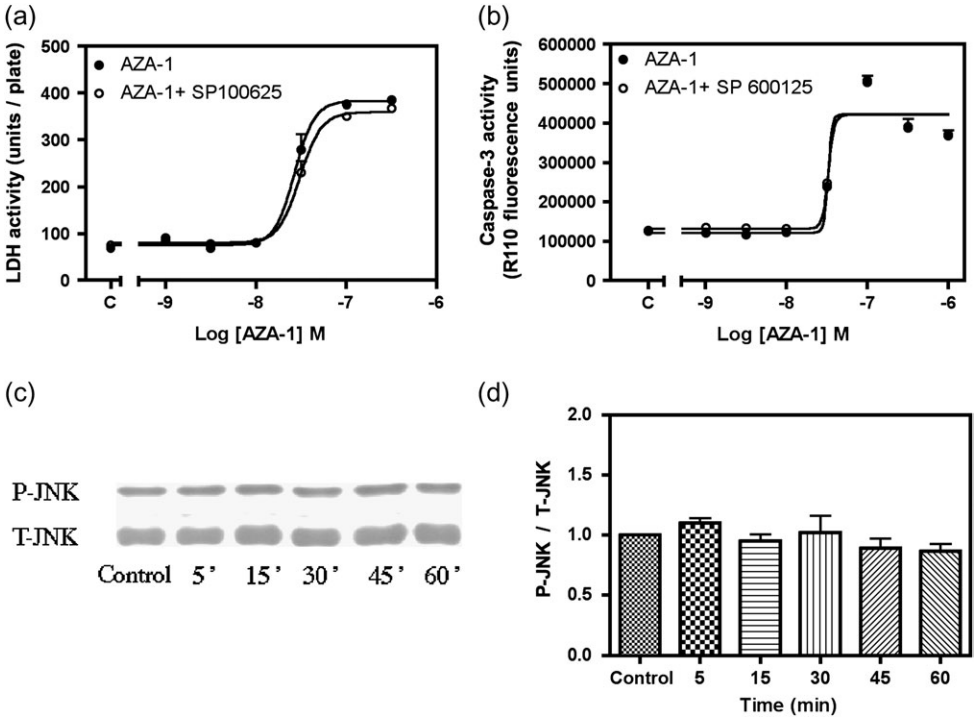

FIG. 8. (a) Lack of effect of the JNK inhibitor, SP 600125 (10μM), on AZA-1–induced LDH efflux. (b) Lack of effect of SP 600125 (10μM) on AZA-1–induced caspase-3 activity. These data were obtained from three independent experiments performed in triplicate. (c) Representative Western blot for the lack of influence of AZA-1 (1μM) on JNK phosphorylation. (d) Quantification of JNK phosphorylation after exposure of neocortical cells to AZA-1 (1μM). The data were pooled from three independent experiments.

in breathing (McMahon and Silke, 1996). An earlier report evaluated a range of mammalian cell lines for sensitivity to AZA-induced cytotoxicity (Twiner *et al*., 2005). Although a 24-h exposure to AZA-1 caused significant cytotoxicity in all cell lines tested except A549 lung epithelial cells, only Jurkat T lymphocytes and GH_4C_1 pituitary cells were sufficiently sensitive to permit EC_{50} determination (Twiner *et al*., 2005). The EC_{50} values for the latter two cell types were in the nanomolar range: again indicating that AZA-1 is a potent toxin.

During the process of apoptosis, cells undergo several characteristic morphological changes, such as cell shrinkage, nuclear/chromatin condensation, membrane blebbing, and formation of apoptotic bodies (Kerr *et al*., 1972; Mills *et al*., 1999). One of the mechanisms responsible for apoptotic morphological changes is the activation of proteases, such as the caspase family, whose activation is considered to be an early marker of apoptosis (Maravei *et al*., 1997). Vilarino *et al*. (2007) previously reported that AZA-1 stimulated caspase activity, including caspase-1 and caspase-3 to -9 in neuroblastoma cells, suggesting that AZA-1 may produce apoptotic cell death in these cells. We have confirmed the ability of AZA-1 treatment to produce neuronal apoptosis as evidenced by both nuclear condensation and stimulation of caspase-3 activity in neocortical neurons. These data extend previous reports of caspase activation in neuroblastoma cells to neocortical neurons in primary culture.

An interesting feature of our results with AZAs is that AZA-1–induced neurotoxicity includes both necrotic and apoptotic processes in neocortical neurons and that these two distinct types of cell death may occur simultaneously. This type of hybrid cell death has been reported previously in neocortical neurons where the Na^+, K^+-ATPase inhibitor, ouabain, produced neurotoxicity through both necrosis and apoptosis simultaneously (Xiao *et al*., 2002; Yu, 2003). While an AZA-1 inhibition of Na^+, K^+-ATPase cannot presently be ruled out, one difference between the neurotoxic response to AZA-1 and ouabain is that nifedipine afforded protection from ouabain but not AZA-1–induced neurotoxicity (Xiao *et al*., 2002).

Consistent with the demonstration that the full structure is required for AZA to produce neurotoxicity in CGCs (Vale *et al*., 2007b), we also demonstrated that AZA-1, AZA-2 (8-methyl-azaspracid), and AZA-3 (22-demethyl-azaspiracid), but not fragments containing either the ABCDE or the FGHI domain alone, elevated LDH efflux and stimulated caspase-3 activity. The similar potency on LDH efflux of AZA-1 and AZA-2 accords with the data reported previously in neuroblastoma cells (Vilarino *et al*., 2008). Additionally, we provide the first demonstration that AZA-3 is a neurotoxin being somewhat more potent than AZA-1. Collectively, these structure-activity data suggest that the C22 methyl moiety, but not the C8 methyl moiety, appear to affect the potency of AZA-induced toxicity in neocortical neurons.

Our results also demonstrated that AZA-1 was a potent inhibitor of spontaneous Ca^{2+} oscillations in neocortical neurons. Synchronization of Ca^{2+} oscillations in neurons is considered to result from synaptic communication in a neuronal network. It has been previously demonstrated that AZA-1 inhibited bioelectrical activity of a spinal cord neuronal network (Kulagina *et al*., 2006). Considered together these data suggest that this toxin affects synaptic transmission in neuronal networks (Kulagina *et al*., 2006).

Our results indicate that the molecular targets for inhibition of spontaneous Ca^{2+} oscillations and neurotoxicity may differ. This is based on the observation that fragments 11, 12, 14, and 15 inhibited spontaneous Ca^{2+} oscillation in neocortical neurons, whereas they were inactive in the LDH efflux assay. These structure-activity data demonstrate that fragments 11 (natural FGHI-(*S*)-phenyl glycine methyl ester), 12 (natural FGHI-(*R*)-phenyl glycine methyl ester), 14 (*ent*-FGHI-(*S*)-phenyl glycine methyl ester), and 15 (*ent*-FGHI-(*R*)-phenyl glycine methyl ester), but not compounds 10 (natural FGHI) and 13 (*ent*-FGHI), were potent inhibitors of spontaneous Ca^{2+} oscillations. These results suggest that the phenyl glycine methyl ester moiety attached to the FGHI domain was necessary to produce inhibitory effects on spontaneous Ca^{2+} oscillations. Compounds 12 and 15 were, respectively, significantly more potent than fragments 11 and 14, suggesting that compounds with the *R* configuration were more potent than compounds with the *S* configuration. These data therefore reveal stereoselectivity of AZA fragments interacting with an unknown target. Additionally, compounds 11 and 12 were also significantly more potent than compounds 14 and 15, suggesting that the natural FGHI backbone afforded greater potency than *ent*-FGHI backbone for these compounds as inhibitors of spontaneous Ca^{2+} oscillations. AZA-3 was found to be more potent than AZA-1 on spontaneous Ca^{2+} oscillation, whereas AZA-2 has similar potency to AZA-1. This profile is therefore similar to that observed with LDH efflux and again suggests that the C22, but not the C8 methyl moiety, influences the affinity for AZA binding to the target responsible for inhibition of spontaneous Ca^{2+} oscillations.

In contrast to previous reports demonstrating that AZAs composed of either the full ring domain structure or the fragments containing only the ABCD/ABCDE rings stimulated Ca^{2+} influx in CGCs and lymphocytes (Roman *et al*., 2002; Vale *et al*., 2007a), we found no evidence for AZAs or ABCDE domain induced stimulation of Ca^{2+} influx in neocortical neurons. This discrepancy may be due to either the different experimental protocols for manipulation of extracellular Ca^{2+} or the use of different cell types.

Our results demonstrated that Ac-DEVD-CMK (50μM), a permeable and irreversible caspase-3 inhibitor, efficiently suppressed AZA-1–induced caspase-3 activation and produced a partial attenuation of AZA-1–induced cell death in neocortical neurons. These data therefore demonstrate the involvement of caspase-3 activity in AZA-1–induced neurotoxicity. Moreover,

the broad-spectrum caspase inhibitor, Z-VAD-FMK, produced nearly complete suppression of both AZA-1–induced LDH efflux and nuclear condensation. These data indicate that, in addition to caspase-3, other caspases are involved in AZA-1–induced neurotoxicity in neocortical neurons.

Increasing evidence implicates the JNK pathway as an important mediator of cell death in many cell populations. AZA-1 has been demonstrated to stimulate JNK phosphorylation, and the JNK inhibitor, SP 600125, completely blocked AZA-1–induced neurotoxicity in CGCs (Vale *et al*., 2007b). These data suggested the involvement of JNK activity in AZA-1–induced neurotoxicity in CGCs. In contrast to the data with CGCs, we found that AZA-1 did not affect JNK phosphorylation in neocortical neurons. Additionally, the JNK kinase inhibitor SP 600125 was without effect on AZA-1–induced neurotoxicity. Considered together, these data suggest that a JNK kinase pathway is not involved in AZA-1–induced neurotoxicity in neocortical neurons. Because substantial differences exist in the network properties between neocortical and CGC cultures, one must be careful not to assume that these systems will respond identically to neurotoxins, such as AZAs.

In summary, we have demonstrated that AZA-1 produced neocortical neuronal death through both apoptotic and necrotic mechanisms. Moreover, AZAs inhibited spontaneous Ca^{2+} oscillations in neocortical neurons. The evaluation of structure-activity relationships for an array of AZA analogs demonstrated that distinct molecular targets are responsible for inhibition of spontaneous Ca^{2+} oscillations and neurotoxicity. A pharmacologic evaluation excluded VGSCs, NMDA receptors, and L-type Ca^{2+} channels as potential targets for AZA-induced neurotoxicity. Although the molecular target for AZA-induced neurotoxicity remains to be established, our results demonstrate that neurotoxicity is dependent on caspase activation. Further studies are required to delineate the upstream signaling pathways for caspase activation and to define the molecular target(s) for these neurotoxins.

SUPPLEMENTARY DATA

Supplementary data are available online at http://toxsci.oxfordjournals.org/.

FUNDING

National Institutes of Health (NS053398 to T.F.M.; ES 01331402 and ES 01331403 to K.C.N.), the National Center for Research Resources (G20 RR024001), and the National Science Foundation for a predoctoral fellowship to M.O.F. The content is solely the responsibility of the authors and does not necessarily represent the official views of the National Center for Research Resources or the National Institutes of Health.

REFERENCES

Alfonso, A., Roman, Y., Vieytes, M. R., Ofuji, K., Satake, M., Yasumoto, T., and Botana, L. M. (2005). Azaspiracid-4 inhibits Ca2+ entry by stored operated channels in human T lymphocytes. *Biochem. Pharmacol.* **69,** 1627–1636.

Cao, Z., George, J., Baden, D. G., and Murray, T. F. (2007). Brevetoxin-induced phosphorylation of Pyk2 and Src in murine neocortical neurons involves distinct signaling pathways. *Brain Res.* **1184,** 17–27.

Dravid, S. M., and Murray, T. F. (2004). Spontaneous synchronized calcium oscillations in neocortical neurons in the presence of physiological [Mg(2+)]: involvement of AMPA/kainate and metabotropic glutamate receptors. *Brain Res.* **1006,** 8–17.

Furey, A., Brana-Magdalena, A., Lehane, M., Moroney, C., James, K. J., Satake, M., and Yasumoto, T. (2002). Determination of azaspiracids in shellfish using liquid chromatography/tandem electrospray mass spectrometry. *Rapid Commun. Mass Spectrom.* **16,** 238–242.

Gu, X., and Spitzer, N. C. (1995). Distinct aspects of neuronal differentiation encoded by frequency of spontaneous Ca2+ transients. *Nature* **375,** 784–787.

Ito, E., Satake, M., Ofuji, K., Higashi, M., Harigaya, K., McMahon, T., and Yasumoto, T. (2002). Chronic effects in mice caused by oral administration of sublethal doses of azaspiracid, a new marine toxin isolated from mussels. *Toxicon* **40,** 193–203.

Ito, E., Satake, M., Ofuji, K., Kurita, N., McMahon, T., James, K., and Yasumoto, T. (2000). Multiple organ damage caused by a new toxin azaspiracid, isolated from mussels produced in Ireland. *Toxicon* **38,** 917–930.

James, K. J., Furey, A., Lehane, M., Ramstad, H., Aune, T., Hovgaard, P., Morris, S., Higman, W., Satake, M., and Yasumoto, T. (2002). First evidence of an extensive northern European distribution of azaspiracid poisoning (AZP) toxins in shellfish. *Toxicon* **40,** 909–915.

Kerr, J. F., Wyllie, A. H., and Currie, A. R. (1972). Apoptosis: a basic biological phenomenon with wide-ranging implications in tissue kinetics. *Br. J. Cancer* **26,** 239–257.

Koh, J. Y., and Choi, D. W. (1987). Quantitative determination of glutamate mediated cortical neuronal injury in cell culture by lactate dehydrogenase efflux assay. *J. Neurosci. Methods* **20,** 83–90.

Kulagina, N. V., Twiner, M. J., Hess, P., McMahon, T., Satake, M., Yasumoto, T., Ramsdell, J. S., Doucette, G. J., Ma, W., and O'Shaughnessy, T. J. (2006). Azaspiracid-1 inhibits bioelectrical activity of spinal cord neuronal networks. *Toxicon* **47,** 766–773.

Magdalena, A. B., Lehane, M., Krys, S., Fernandez, M. L., Furey, A., and James, K. J. (2003). The first identification of azaspiracids in shellfish from France and Spain. *Toxicon* **42,** 105–108.

Maravei, D. V., Trbovich, A. M., Perez, G. I., Tilly, K. I., Banach, D., Talanian, R. V., Wong, W. W., and Tilly, J. L. (1997). Cleavage of cytoskeletal proteins by caspases during ovarian cell death: evidence that cell-free systems do not always mimic apoptotic events in intact cells. *Cell Death Differ.* **4,** 707–712.

McMahon, T., and Silke, J. (1996). Winter toxicity of unknown aetiology in mussels. *Harmful Algae News* **14,** 2.

Mills, J. C., Stone, N. L., and Pittman, R. N. (1999). Extranuclear apoptosis. The role of the cytoplasm in the execution phase. *J. Cell Biol.* **146,** 703–708.

Nicolaou, K. C., Chen, D. Y., Li, Y., Uesaka, N., Petrovic, G., Koftis, T. V., Bernal, F., Frederick, M. O., Govindasamy, M., Ling, T., *et al.* (2006a).

Total synthesis and structural elucidation of azaspiracid-1. Synthesis-based analysis of originally proposed structures and indication of their non-identity to the natural product. *J. Am. Chem. Soc.* **128,** 2258–2267.

Nicolaou, K. C., Frederick, M. O., Petrovic, G., Cole, K. P., and Loizidou, E. Z. (2006b). Total synthesis and confirmation of the revised structures of azaspiracid-2 and azaspiracid-3. *Angew. Chem. Int. Ed. Engl.* **45,** 2609–2615.

Nicolaou, K. C., Koftis, T. V., Vyskocil, S., Petrovic, G., Ling, T., Yamada, Y. M., Tang, W., and Frederick, M. O. (2004a). Structural revision and total synthesis of azaspiracid-1, part 2: definition of the ABCD domain and total synthesis. *Angew. Chem. Int. Ed. Engl.* **43,** 4318–4324.

Nicolaou, K. C., Koftis, T. V., Vyskocil, S., Petrovic, G., Tang, W., Frederick, M. O., Chen, D. Y., Li, Y., Ling, T., and Yamada, Y. M. (2006c). Total synthesis and structural elucidation of azaspiracid-1. Final assignment and total synthesis of the correct structure of azaspiracid-1. *J. Am. Chem. Soc.* **128,** 2859–2872.

Nicolaou, K. C., Pihko, P. M., Bernal, F., Frederick, M. O., Qian, W., Uesaka, N., Diedrichs, N., Hinrichs, J., Koftis, T. V., Loizidou, E., *et al.* (2006d). Total synthesis and structural elucidation of azaspiracid-1. Construction of key building blocks for originally proposed structure. *J. Am. Chem. Soc.* **128,** 2244–2257.

Nicolaou, K. C., Vyskocil, S., Koftis, T. V., Yamada, Y. M., Ling, T., Chen, D. Y., Tang, W., Petrovic, G., Frederick, M. O., Li, Y., *et al.* (2004b). Structural revision and total synthesis of azaspiracid-1, part 1: intelligence gathering and tentative proposal. *Angew. Chem. Int. Ed. Engl.* **43,** 4312–4318.

Nunez, L., Sanchez, A., Fonteriz, R. I., and Garcia-Sancho, J. (1996). Mechanisms for synchronous calcium oscillations in cultured rat cerebellar neurons. *Eur. J. Neurosci.* **8,** 192–201.

Ofuji, K., Satake, M., McMahon, T., James, K. J., Naoki, H., Oshima, Y., and Yasumoto, T. (2001). Structures of azaspiracid analogs, azaspiracid-4 and azaspiracid-5, causative toxins of azaspiracid poisoning in Europe. *Biosci. Biotechnol. Biochem.* **65,** 740–742.

Ogura, A., Iijima, T., Amano, T., and Kudo, Y. (1987). Optical monitoring of excitatory synaptic activity between cultured hippocampal neurons by a multi-site Ca2+ fluorometry. *Neurosci. Lett.* **78,** 69–74.

Roman, Y., Alfonso, A., Louzao, M. C., de la Rosa, L. A., Leira, F., Vieites, J. M., Vieytes, M. R., Ofuji, K., Satake, M., Yasumoto, T., *et al.* (2002). Azaspiracid-1, a potent, nonapoptotic new phycotoxin with several cell targets. *Cell. Signal.* **14,** 703–716.

Roman, Y., Alfonso, A., Vieytes, M. R., Ofuji, K., Satake, M., Yasumoto, T., and Botana, L. M. (2004). Effects of azaspiracids 2 and 3 on intracellular cAMP, [Ca2+], and pH. *Chem. Res. Toxicol.* **17,** 1338–1349.

Satake, M., Ofuji, K., Naoki, H., James, K. J., Furey, A., McMahon, T., Silke, J., and Yasumoto, T. (1998). Azaspiracid, a new marine toxin having unique spiro ring assemblies, isolated from Irish mussels, Mytilus edulis. *J. Am. Chem. Soc.* **120,** 9967–9968.

Spitzer, N. C., Olson, E., and Gu, X. (1995). Spontaneous calcium transients regulate neuronal plasticity in developing neurons. *J. Neurobiol.* **26,** 316–324.

Twiner, M. J., Hess, P., Dechraoui, M. Y., McMahon, T., Samons, M. S., Satake, M., Yasumoto, T., Ramsdell, J. S., and Doucette, G. J. (2005). Cytotoxic and cytoskeletal effects of azaspiracid-1 on mammalian cell lines. *Toxicon* **45,** 891–900.

Vale, C., Gomez-Limia, B., Nicolaou, K. C., Frederick, M. O., Vieytes, M. R., and Botana, L. M. (2007a). The c-Jun-N-terminal kinase is involved in the neurotoxic effect of azaspiracid-1. *Cell. Physiol. Biochem.* **20,** 957–966.

Vale, C., Nicolaou, K. C., Frederick, M. O., Gomez-Limia, B., Alfonso, A., Vieytes, M. R., and Botana, L. M. (2007b). Effects of azaspiracid-1, a potent cytotoxic agent, on primary neuronal cultures. A structure-activity relationship study. *J. Med. Chem.* **50,** 356–363.

Vilarino, N., Nicolaou, K. C., Frederick, M. O., Cagide, E., Alfonso, C., Alonso, E., Vieytes, M. R., and Botana, L. M. (2008). Azaspiracid substituent at C1 is relevant to in vitro toxicity. *Chem. Res. Toxicol.* **21,** 1823–1831.

Vilarino, N., Nicolaou, K. C., Frederick, M. O., Vieytes, M. R., and Botana, L. M. (2007). Irreversible cytoskeletal disarrangement is independent of caspase activation during in vitro azaspiracid toxicity in human neuroblastoma cells. *Biochem. Pharmacol.* **74,** 327–335.

Xiao, A. Y., Wei, L., Xia, S., Rothman, S., and Yu, S. P. (2002). Ionic mechanism of ouabain-induced concurrent apoptosis and necrosis in individual cultured cortical neurons. *J. Neurosci.* **22,** 1350–1362.

Yu, S. P. (2003). Na(+), K(+)-ATPase: the new face of an old player in pathogenesis and apoptotic/hybrid cell death. *Biochem. Pharmacol.* **66,** 1601–1609.